Investigating the role of Bcl-2 protein, Noxa, in the metabolic reprogramming, differentiation and apoptosis of CD8$^+$ T cells during the immune response

A thesis submitted to the Graduate School

of the

University of Minnesota

By

Tingyuan Yang

In partial fulfillment of the requirements for the degree of

Master of Science

Adviser: Dr. Ameeta Kelekar

July 2021

Acknowledgement

I would like to thank my advisor, Dr. Ameeta Kelekar, who provided invaluable advice and helped me during difficult periods. I want to thank everyone in the Kelekar lab, Karl Krecke and Sarah Elmer, for helping and taking care of me. I would like to acknowledge my committee members, Dr. Christopher Pennell and Dr. Kristin Hogquist, who gave me positive guidance and feedback and helped me in completing the defense. Last but not least, I want to thank my parents who have supported and encouraged me all the time.

Abstract:

Human Noxa was previously shown to have both pro-apoptotic and pro-growth functions in leukemic and primary T cells. Noxa was also shown to be required for the switch to glutamine metabolism of antigen stimulated CD8$^+$ T cells. Our studies show that Noxa is consistently induced in normal human CD8$^+$T cells upon stimulation and remains highly expressed during differentiation and through the onset of apoptosis. Memory-like CD8$^+$ T cells recovered at the end of the immune response no longer express Noxa but exhibit robust induction of the protein upon re-stimulation. CD8$^+$ T cells lacking Noxa expression showed an overall reduced dependence on glutamine and higher viability at the end of the immune response. Our studies have offered valuable insights into metabolic pathways that regulate cell fate in human CD8$^+$ T lymphocytes and a deeper understanding of Noxa's role in regulating T cell metabolism and will help evaluate Noxa's potential for immunotherapy.

Contents:

List of Figures and Tables:

Chapter 1: Introduction

Human Noxa, a phorbol-12-Myristate-13-Acetate-Induced Protein [1], is a BH3-only member of the Bcl-2 family of apoptosis regulator proteins. BH3-only proteins are pro-apoptotic and promote apoptosis by binding and inhibiting pro-survival Bcl-2 family members [2, 3]. Noxa promotes apoptosis via interaction with its specific binding partner, Mcl-1, through its BH3 domain. Human Noxa, with only 54 residues and one BH3 domain (Fig 1.1), is the smallest known Bcl-2 protein, different from mouse Noxa, which is a larger protein with 103 residues and two BH3 domains [4].

Fig 1.1| Amino acid sequence of hNoxa. The BH3 domain (LRRFGDK) and putative kinase substrate motif (QPSPARA) are underlined. Copy right: doi:10.1016/j.molcel.2010.11.035

Human Noxa is constitutively expressed in human cancer cells of hematopoietic origin and was shown to function both as a growth-promoter and a pro-apoptotic protein in T leukemia cells [5, 6]. The protein is phosphorylated on a serine residue(S^{13}) in proliferating Jurkat cells and the phosphorylation, which is glucose-dependent, prevents Noxa from activating apoptosis by effectively masking the pro-apoptotic BH3 domain and rendering it inaccessible to Mcl-1 (Fig. 1.2)[6].

Kinase inhibitors or glucose limitation cause Noxa to be dephosphorylated and to promote apoptosis by allowing the interaction of Mcl-1 with the Noxa BH3 domain [7]. While Noxa can be immunoprecipitated from extracts of Jurkat T-ALL cells undergoing apoptosis, the pro-survival phosphorylated form of Noxa is found localized within a large, stable, multiprotein cytosolic complex, that also includes Mcl-1, and is inaccessible for immunoprecipitation in proliferating cells [6].

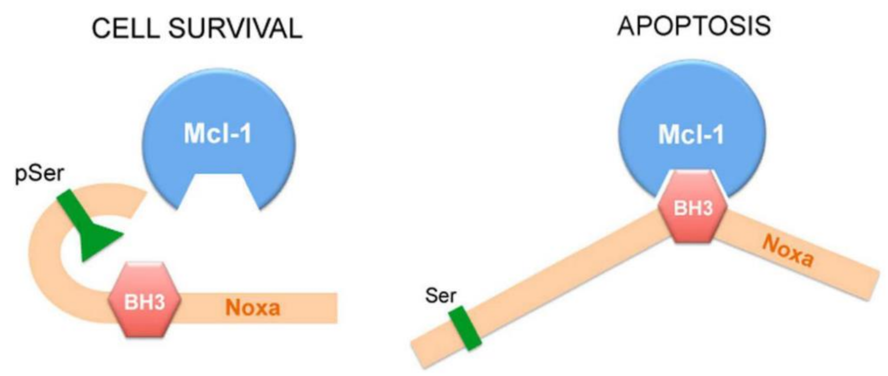

Fig 1.2| Regulation of the Noxa-Mcl-1 interaction via Serine 13 phosphorylation. Shown in the figure is a simplified cartoon demonstrating how the partial masking of the BH3 domain resulting from phosphorylation of Ser13 could inhibit the interaction of Noxa with Mcl-1. Copy right: doi:10.1038/srep14557

In its pro-survival form, Noxa was shown to promote growth as a metabolic regulator. Noxa enhanced aerobic glycolysis and increased glucose consumption and lactate production in Jurkat T-ALL cells [6]. Over-expression of the protein in T leukemia cells led to a reduction in the use of glucose, and an increase in glutaminolysis and the use of glutamine carbons for mitochondrial oxidative phosphorylation (OXPHOS) in the TCA cycle [8]. Most notably, it was also shown that the Noxa protein was rapidly induced in normal human T cells upon antigenic stimulation in vitro and was also phosphorylated in a glucose-dependent manner in the activated cells [6, 9].

T lymphocytes play a dominant role in mediating immune response when faced with pathogen invasion. Naïve lymphocytes circulate in the body in a resting state but, upon recognition of foreign antigen and appropriate co-stimulatory signals, become activated and go through a rapid proliferative burst before assuming effector functions directed at killing the target 'invading' organism or cancer cell [10, 11]. Ultimately, T lymphocytes differentiate into different subtypes, secreting cytokines and conducting distinct functions to maintain homeostasis in the immune system (Fig1.3. a.). Cytotoxic T cells (CTLs), activated $CD8^+$ T cells, mediate the elimination of antigens through inducing apoptosis triggered by the releasing of cytolytic granules, which initiate the perforin-granzyme pathway and FAS-FAS ligand pathway [12, 13]. Helper T cells, a subset of activated $CD4^+$ T cells, secrete cytokines to activate macrophages, produce antibodies and suppress infection [14, 15]. To maintain homeostasis, regulatory T cells, a subset of activated $CD4^+$ T cells, play a significant role in inhibiting the activity of effector T cells and suppressing immunity (Fig 1.3. b.)[16, 17]. Once pathogens are eliminated, most effector T cells succumb to apoptosis, while a few are retained as memory cells. A significant factor in regulating the apoptosis process is the BH3-only protein, which can form heterodimeric complexes at the mitochondria with multidomain survival Bcl-2 proteins and promote the release of cytochrome C from mitochondria [18, 19]. It has been well established in mouse T cells that BH3-only proteins, Bim and Puma which show high affinity to several pro-survival Bcl-2-like proteins play prominent roles in apoptosis of immune cells [20, 21]. However, less is known about specific BH3-only proteins that regulate the immune response in human T cells.

It is well documented that metabolism in T lymphocytes is dynamic, modulates the immune response, and is tightly linked to cell function [22, 23]. Prior to TCR/CD28 stimulation, naïve T cells are dependent largely on mitochondrial oxidative phosphorylation (OXPHOS) for ATP generation. After antigenic engagement, activated T lymphocytes switch to aerobic glycolysis, which facilitates the uptake and incorporation of nutrients into biomass to meet the higher demands of rapid expansion and differentiation. However, the signaling pathways that facilitate this shift are poorly understood. The diversion of glucose to biosynthetic pathways increases the demand for amino acids, such as glutamine, for maintaining OXPHOS for energy production, which is crucial for the activation-associated proliferation of effector T cells. By contrast, Treg cells and long-lived memory T cells derive their energy from lipid oxidation (Fig 1.3.).

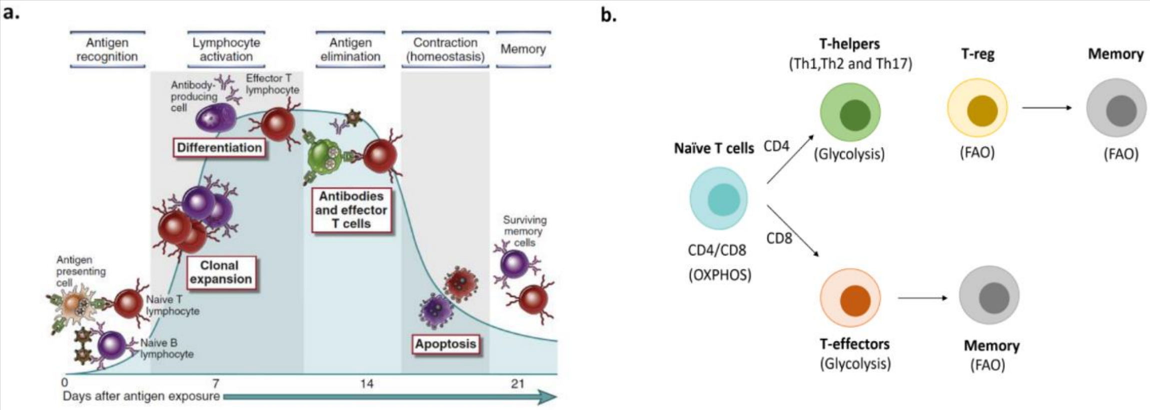

Fig 1.3. The adaptive immune response of human T lymphocytes. a, An adaptive immune response consists of distinct phases, the first three being recognition of antigen, activation of lymphocytes, and the elimination of antigen (the effector phase). The response contracts (declines) as antigen-stimulated lymphocytes die by apoptosis, restoring homeostasis, and the antigen-specific cells that survive are responsible for memory (Copy right: Cellular and Molecular Immunology/Abul K. Abbas, Andrew H. Lichtman, Shiv Pillai ; illustrations by David L. Baker, Alexandra Baker. – 8th edition). **b**, Different classes of lymphcytes and cooresponding primary metabolism pathway in the cells (FAO: Fatty acid oxidation).

We hypothesize that the **BH3-only Noxa is required for the metabolic alterations in human T cells following their activation and modulates both the expansion and the apoptotic phases of an immune response.** This hypothesis is based on the following published[6, 8] and preliminary unpublished [Benson and Kelekar] studies from our lab. Human Noxa can function either as a pro-survival or a pro-apoptotic protein depending on the phosphorylated state of a single serine residue [6, 24]. It promotes both aerobic glycolysis and glutaminolysis in T leukemia cells [6, 8]. It is rapidly induced and phosphorylated in primary human T cells following antigenic stimulation [6][unpublished] (Fig 1.4a). Moreover, Noxa protein induction required glutamine, not glucose, suggesting a role for the protein in the switch from OXPHOS to proliferative, glutamine-dependent, metabolism (Fig 1.4b). Noxa is also predicted to be sequestered in a cytosolic multiprotein particle in actively proliferating primary T cells based on studies in Jurkat cells [6]. The research described in this dissertation will test the above hypothesis, using human CD8$^+$ T cells as models. The working hypothesis is shown in a simplified model in Fig 1.5.

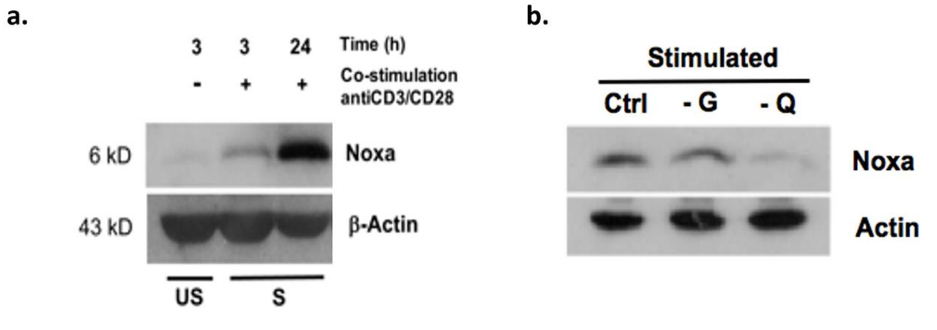

Fig 1.4| Preliminary data in CD3$^+$ T cells. **a,** Noxa expression was induced by the antigenic stimulation in T cells. **b,** The absence of glutamine, rather than glucose, caused a decreased of Noxa expression in stimulated T cells. (G: glucose; Q: glutamine)

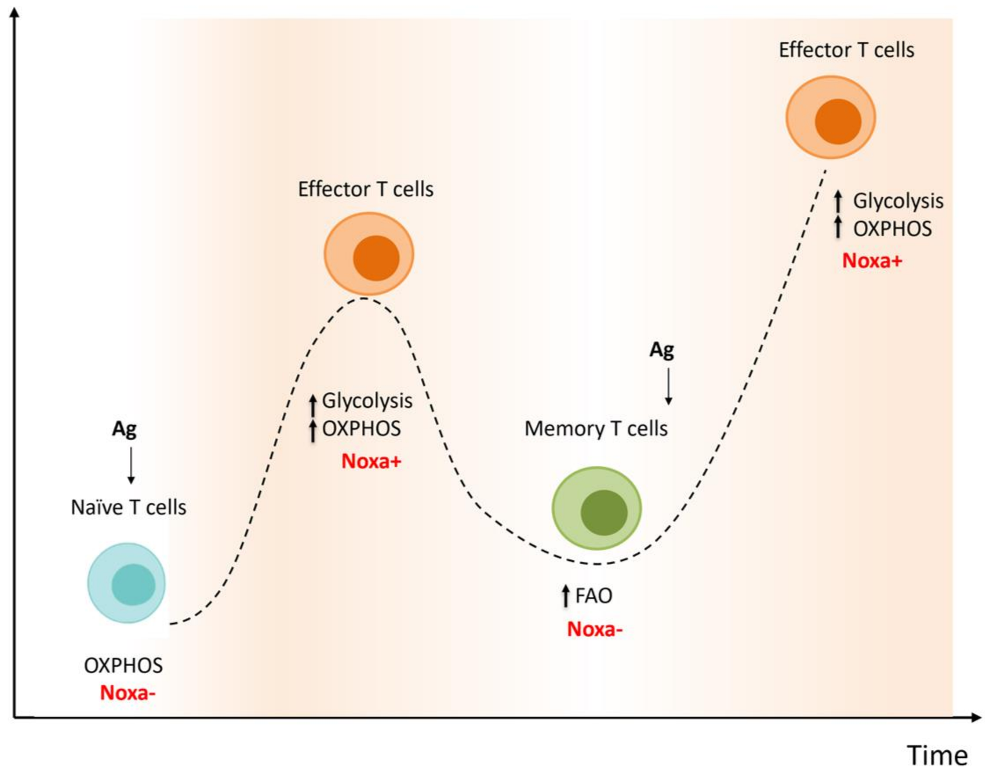

Fig 1.5| Model for Noxa expression during the CD8T cell Immune Response.

Chapter 2: Results

In this study, we test the hypothesis that **BH3-only protein Noxa is required for the metabolic alterations in human CD8$^+$ T cells following their antigenic stimulation and modulates both the expansion and the apoptotic phases of an immune response.**

Rationale: We selected CD8$^+$ T over CD4$^+$ T cells to investigate the role of Noxa in the immune response in vitro. Given that any in vitro model with normal human T cells has its limitations, we surmised that an immune response model with CD8$^+$ T cells would be simpler to set up, as well as to monitor and interpret. It would allow us to follow expression of Noxa through distinct phases of activation (see Figure 1.3a), proliferation, differentiation, apoptosis and, possibly, through memory cell formation, in a single subtype. A similar activation experiment with freshly isolated CD4$^+$ T cells would need to take into account differing fuel and cytokine dependencies and metabolic pathways of the helper subtypes, as well as those of regulatory T cells and would be more challenging to interpret.

Tracking a human CD8$^+$ T cell 'immune response' in vitro – experimental setup

Human CD8$^+$ T cells were isolated from human peripheral blood mononuclear cells (PBMCs) and stimulated with anti-CD3 and anti-CD28 antibodies to model the immune response in vitro. Unstimulated cells and activated cells, harvested at specific time points after stimulation, were evaluated for activation, proliferation, metabolic state and apoptosis, using flow cytometry, western blotting and mitochondrial oxygen consumption rates (Fig.

2.1; Table 2.1).

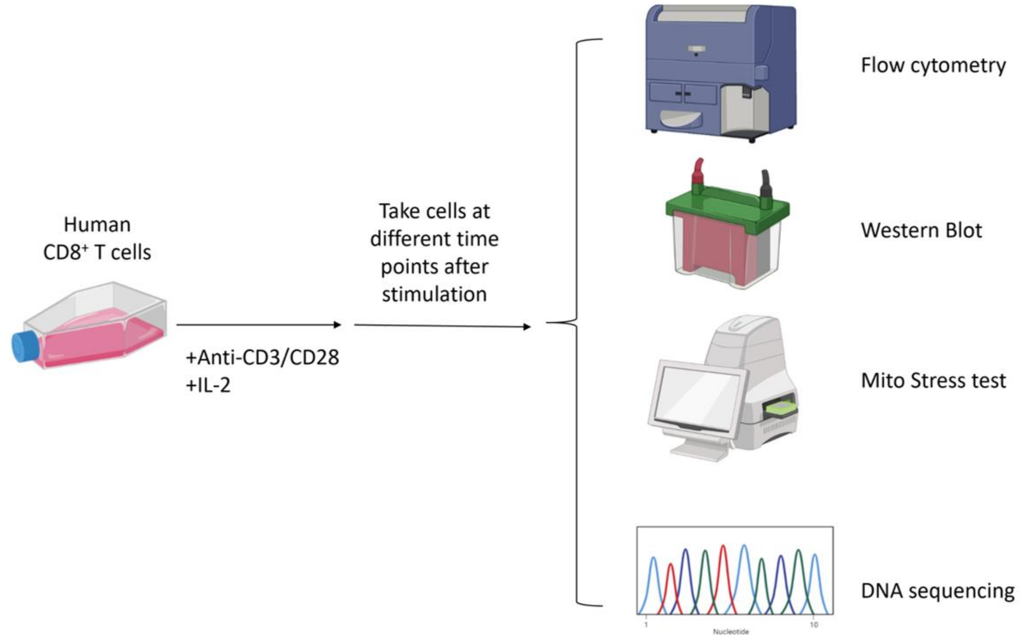

Fig. 2.1| Experimental setup. Readouts for stimulation of human CD8$^+$ T cells in vitro.

	US	20h	40h	d4	d6	d8	d11	d13	d15	Mem-US	20h-re	40h-re	d4-re
Flow cytometry	√	√	√	√	√	√	√	√	√	√	√	√	√
Western blot	√		√	√	√	√	√	√	√	√	√	√	√
Immunoprecipitation	√		√	√	√	√							
Metabolism test	√	√								√	√		
ATAC-seq	√		√		√					√	√		

Table 2.1| Immune Response Experiment. CD8+T cells (US) were co-stimulated with anti-CD3/CD28 antibodies and samples were collected every 2 days for flow cytometric evaluation and lysate preparation. Samples for metabolic phenotyping and oxygen consumption measurements and for ATAC-seq were collected less frequently and at different times (US: unstimulated cells; MEM-US: memory unstimulated cells; re: re-stimulation).

Flow cytometry. Cells were collected every 48h for analysis with flow cytometry. Shown in the Table 2.2 below are specific marker antibodies and fluorescent reagents that were used for identifying viable cells and characterizing their differentiated state. All the data were recorded on the same flow cytometer for each donor for the different time points. To quantify the data, we compared the mean fluorescence intensity (MFI) and displayed the data as fold change in MFI at the different time points over that of unstimulated cells.

Western Blotting. Cells were collected at the same time for making whole cell lysates for western blotting and, less frequently, for generating lysates for immunoprecipitations with Noxa antibody. After collecting all samples from different time points during the immune response, lysates and immunoprecipitated samples were assessed by western blot. Protein expression has been tested in this manner with three independent healthy donors with similar results, although only one representative sample is shown.

Fluorescent Markers and Antibodies	Marker for -
Zombie NIR	Dead cell
CD69	T cell early activation
CD25	T cell early activation
CD62L	Naïve T cells and memory T cells
CD107	Degranulation of CTLs
HLA-DR	Late activation in CTLs
CD45RA	Naïve T cells
CD45RO	Memory T cells
Annexin V	Apoptotic cell
7-AAD	Dead cell
TMRE (tetramethylrhodamine ethyl ester)	Mitochondrial transmembrane potential
CellTrace Violet	Cell proliferation

Table 2.2| Markers and representative function used for flow cytometric evaluation.

Metabolic phenotyping and Spare Respiratory Capacity. The oxygen consumption rate (OCR) of $CD8^+$ T cells before and 48h after stimulation/re-stimulation was measured in a Seahorse XFe96 Extracellular flux analyzer. Spare respiratory capacity (SRC) is a robust functional parameter to assess mitochondrial fitness and represents the difference between the max and basal OCRs.

Memory T cell evaluation and restimulation. The generation of $CD8^+$ memory- like T cells was assessed as part of the immune response experiment. A portion of the stimulated cell population was set aside at the start of the experiment and allowed to expand unperturbed until day 14 (d14) after stimulation. The viable cells remaining after a Ficoll density gradient centrifugation, were designated as the human $CD8^+$ memory like unstimulated T cells (Mem-US) and were restimulated with anti-CD3 and anti-CD28 antibodies and again, evaluated by western blot, flow cytometry and a Seahorse mitochondrial fitness test.

ATAC-Seq. To assess *Noxa* gene promoter activity during the immune response expression we turned to ATAC-seq (Assay for Transposase-accessible Chromatin with high-throughput Sequencing) a simple method to detect chromatin accessibility across the genome. The ATAC-Seq method relies on next-generation sequencing (NGS) library construction using the hyperactive transposase Tn5. NGS adapters are loaded onto the transposase, which allows simultaneous fragmentation of chromatin and integration of those adapters into open chromatin regions. The library that is generated is sequenced by NGS and the regions of the genome with open or accessible chromatin are analyzed using bioinformatics. For the ATAC-Seq we isolated genomic DNA from 3 independent donor CD8$^+$ T cells at 5 specific time points (Table 2.1) - unstimulated cells, early activated cells, CTLs (d6), memory T cells (d15) and memory T cells 24h after re-stimulation.

Noxa protein expression is induced in human CD8$^+$ T cells following antigenic stimulation in vitro.

Previous studies had shown that Noxa was rapidly induced in pan (CD3$^+$) T cells upon co-stimulation with anti-CD3/CD28 antibodies (Fig.1.4a). We assessed Noxa expression level in CD8$^+$ T cells after antigenic stimulation. Noxa was not detectable in lysates of unstimulated cells and upregulated within 24h of anti-CD3/CD28 stimulation in vitro (Fig. 2.2 a). Increased expression of the CD69 marker and decreased expression of CD62L around 40h after stimulation confirmed a normal activation pattern (Fig. 2.2 b-c). Activation was accompanied by a significant increase in OCR and SRC of the CD8$^+$ T cells 40h after antigenic stimulation (Fig.2.2 d-e), representative of the increased mitochondrial respiratory activity associated with robust stimulation.

Noxa is highly expressed in the expanding human cytotoxic (CTL)-like effector population and likely contributes to apoptosis

Following the activation phase early after stimulation, human CD8$^+$ T cells undergo rapid expansion before differentiating into cytotoxic T cells (CTLs). Correspondingly, we found CD107α expression was at its highest level on human CD8$^+$ T cells d4 after stimulation (Fig.2.3 a) and observed a steady increase the HLA-DR MFI beginning d4 (Fig.2.3 b).

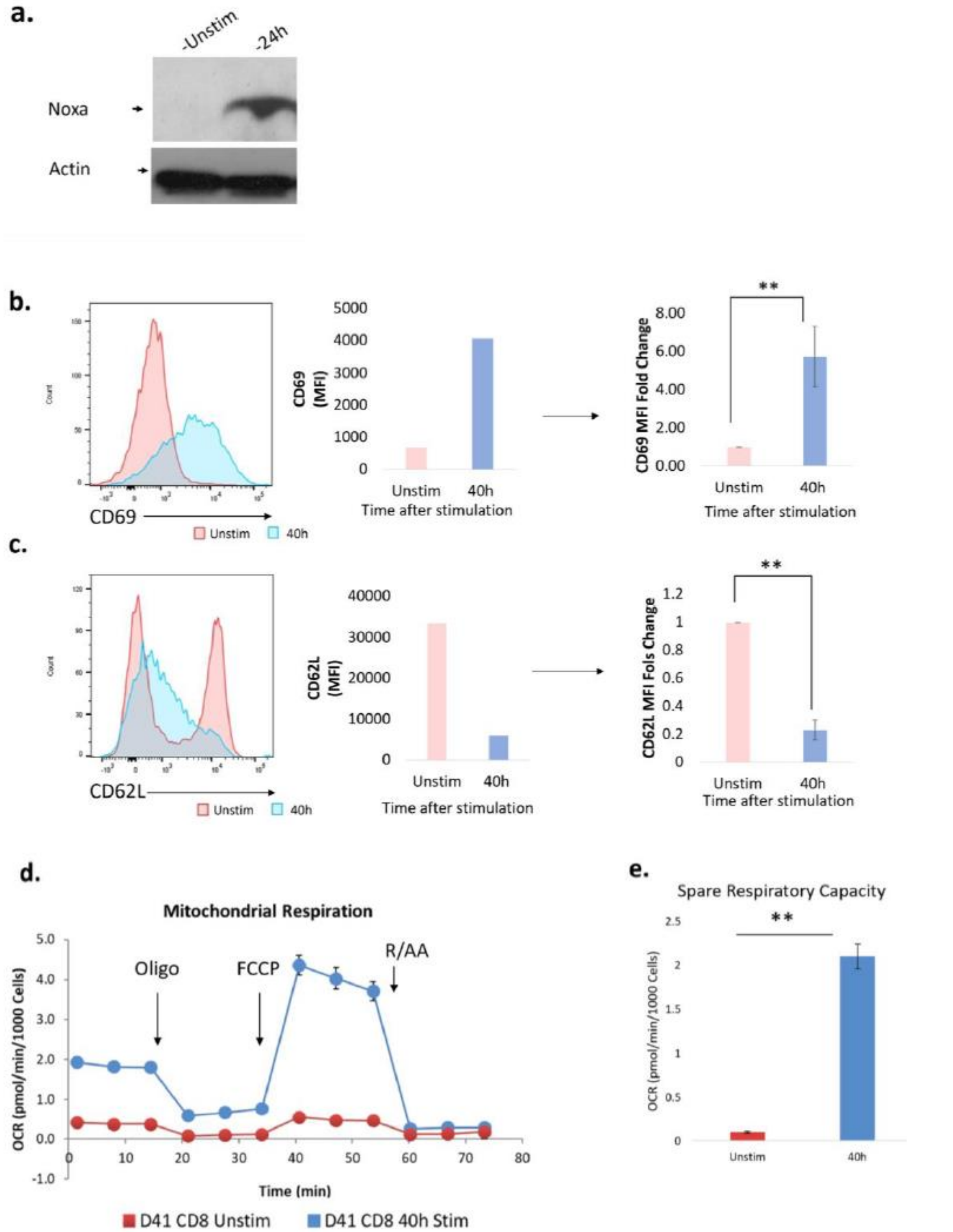

Fig 2.2| Human CD8$^+$ T cells were fully activated 40h after antigenic stimulation. a, Western blotting analysis of 40ug protein extracts from unstimulated and 24h stimulated cells probed for Noxa. β-Actin was used as a loading control.**b,c**, Cells were analyzed at unstimulated status and 40h after stimulation. Representative histograms, MFI and MFI fold change in CD69 and CD62L (data are representative of one (histograms and MFI) or three (MFI fold change) independent experiments. **d,e,** OCR (**d**) and spare respiratory capcity (SCR) (**e**) of human CD8+ T cells in resting and 40h after anti-CD3/CD28 stimulation. Oligo., oligomycin; R/AA, rotenone/antimycin. Sequencing data were from 5 thechnical replicates. Error bars indicate the mean±s.e.m. **p≤0.01.

Rapid proliferation of the activated cells was detectable after day4 of stimulation in vitro and coincided with the appearance of CTL-like differentiation characteristics (Fig.2.3 c).

The onset of apoptosis in the activated, proliferating and differentiating cells in vitro was simultaneously evaluated, using a cleaved caspase-3 marker. We consistently observed an increase in the MFI for cleaved caspase-3 that peaked between d4 and d6 of antigenic stimulation (Fig.2.3 d-e). A second, more sensitive, method, Annexin V-FTIC/7-AAD uptake, for monitoring apoptotic progress, also revealed increased apoptosis after d4 to d6 after stimulation of human $CD8^+$ T cells in vitro (Fig.2.3 f-g). Thus, the $CD8^+$ T cell population that had differentiated into CTL-like cells in vitro entered the apoptotic phase after approximately 4 days of stimulation of anti-CD3/CD28 stimulation.

Noxa was consistently, and highly, expressed in CTL-like cells, closely followed by increased levels of cleaved caspase-3 protein, an indicator of active apoptosis (Fig.2.3 h). Notably, although Noxa was significantly induced within 24 hours of activation, it was accessible for immunoprecipitation only at later times during the human T cells effector phase (Fig.2.3 i). These data support earlier published studies that showed Noxa was phosphorylated and sequestered and inaccessible to immunoprecipitating antibodies in healthy proliferating T leukemia cell extracts but was easily immunoprecipitated as cells became apoptotic following glucose deprivation or activation of a phosphatase. These data tempt us to speculate that, in the late effector phase, Noxa likely interacts with its binding partner, Bcl-2 family protein, Mcl-1, through its BH3 domain to form an accessible complex that promotes apoptosis, although this remains to be directly confirmed.

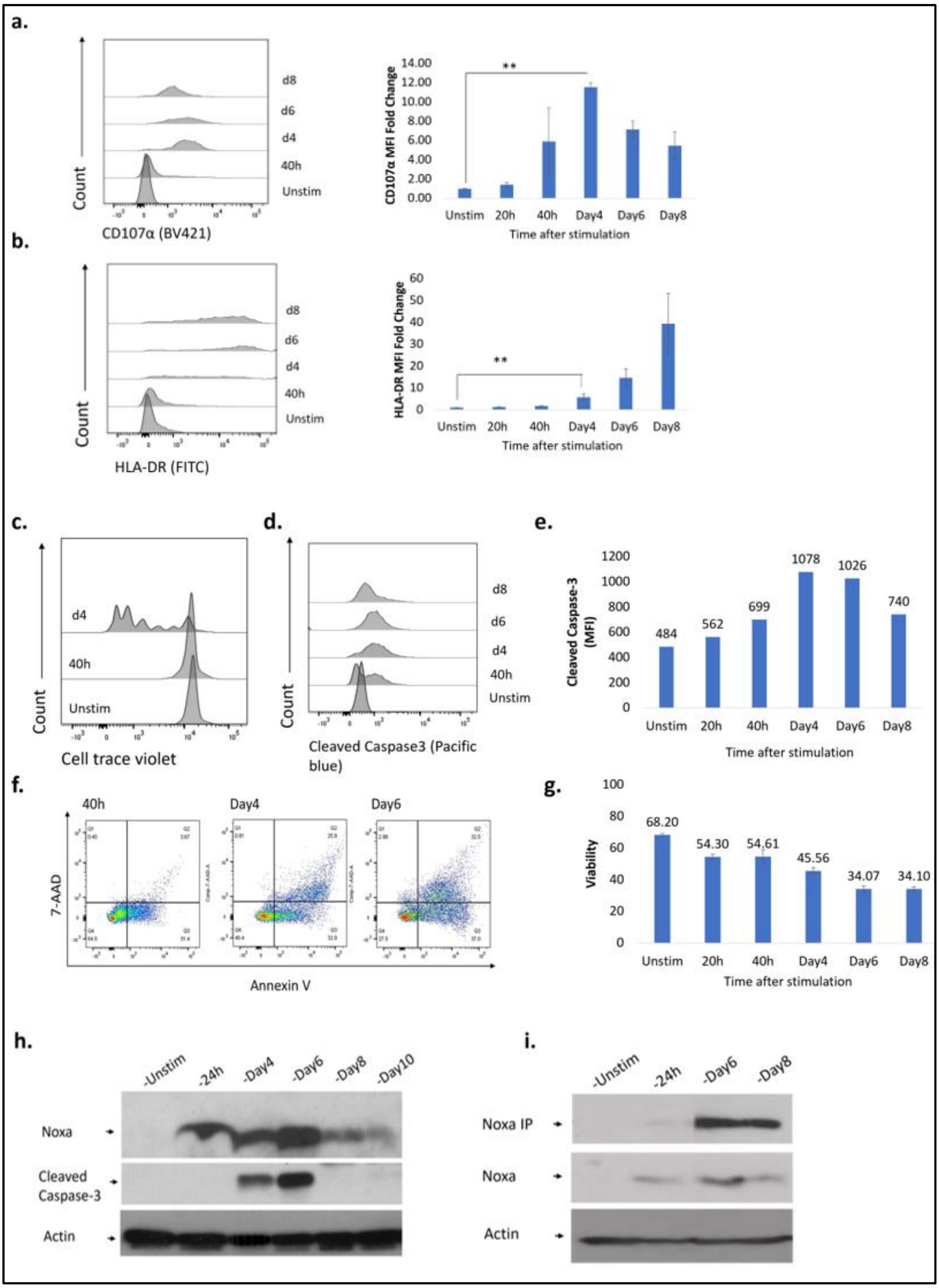

Fig 2.3|. Noxa is highly expressed in human CTLs like cells in vitro. a-e, Cells were analyzed at unstimulated status, 40h and d4 after stimulation. Representative histograms, MFI and MFI fold change in CD107α (**a**), HLA-DR (**b**), CTV (cell trace violet) (**c**) and cleaved caspase-3 (**d,e**) (the MFI level of unstimulated cells was used as standard,1). Data are representative of one (histograms and MFI) or Five (MFI fold change) independent experiments. Error bars indicate the mean±s.e.m. n=5; *p≤0.05; **p≤0.01. **f,g**, Representative dot plot (**f**) and analysis (**g**) of the percentages of annexin V-positive cells. Error bars indicate the mean±s.e.m. n=3. **h,i**, 40ug protein (**h**) made at different time points after stimulation were used for WB and 300ug protein were used for the NoxaIP/western (**i**). Lysate from human CD8+ T cells activation experiment were immunoprecipitated with anti-Noxa mAbs and western blottted for Noxa.

Human CD8$^+$ memory-like T cells do not express Noxa

As we tracked differentiation of the activated CD8$^+$ T cells, we detected the emergence of memory cells. Notably, most of the T cells became CD45RO positive and stayed CD45RO positive after d4 of stimulation (Fig.2.4 a), at the time we detected differentiation of the CD8$^+$ T cells into CTLs or effector-like cells. These observations suggest that CD45RA/CD45RO are not suitable as markers for distinguishing memory T cell generation in vitro. Around d14 following co-stimulation CD69 (Fig.2.4 b), CD107α (Fig.2.4 d) and HLA-DR (Fig.2.4 e) decreased to levels expressed in unstimulated CD8$^+$ T cells, and CD62L expression was restored to levels >4-fold higher than those of unstimulated or naïve cells (Fig.2.4 c). Thus, the human CD8$^+$ T cells had achieved a quiescent status like that of memory T cells around d14 after activation. Consistent with previous data, cleaved caspase3 levels decreased after peaking on d6 after stimulation, returning to levels that suggested low to no apoptotic activity on d14 (Fig.2.4 f). The corresponding viability of human CD8$^+$ T cells slightly increased from 30% to 50% and was maintained at this level (Fig.2.4 g). We conclude that the viable human CD8$^+$ T effector-like cells had acquired a

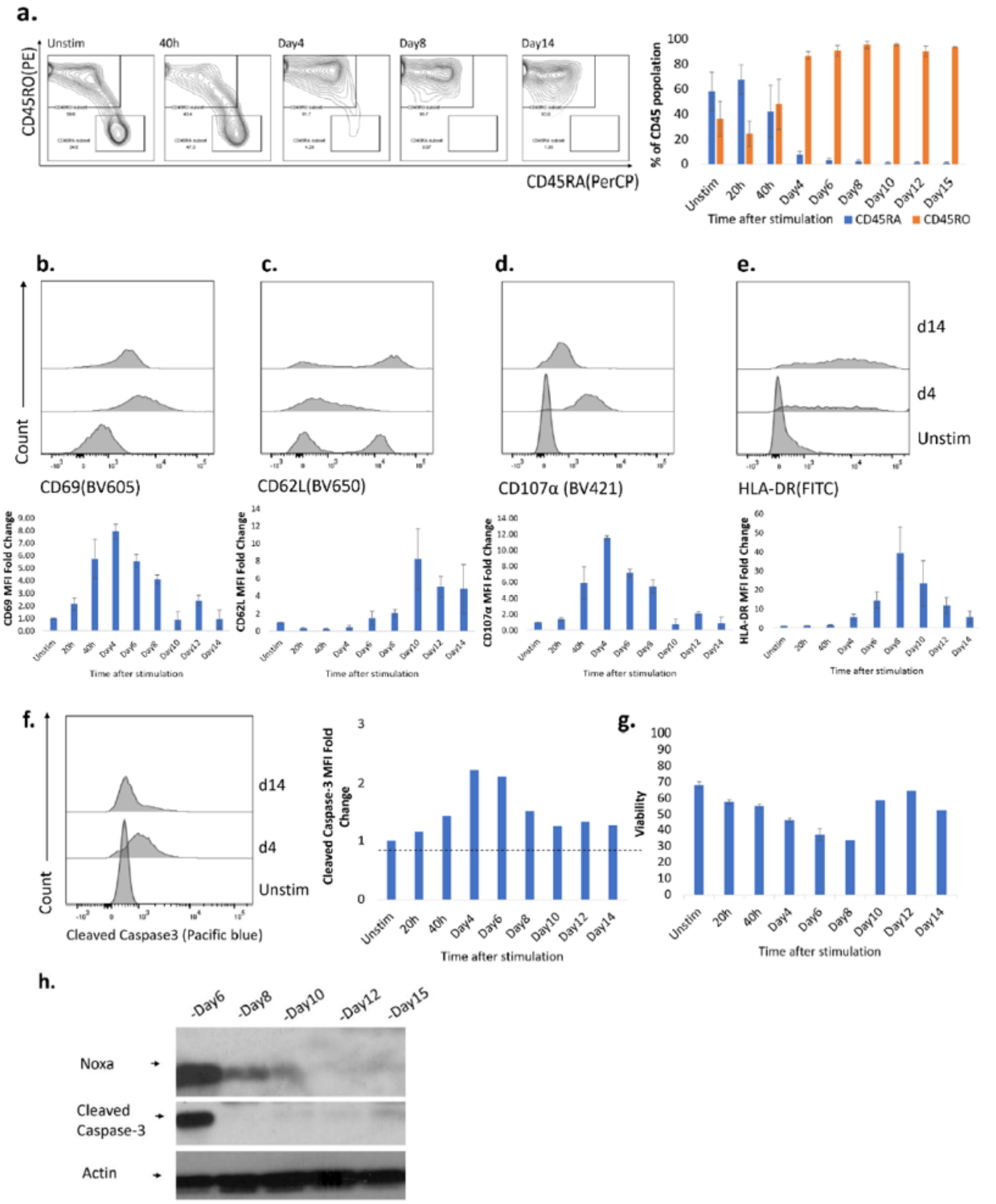

Fig 2.4| Noxa protein is not detected in viable human CD8⁺ memory-like T cells in vitro. a. Representative contour plot and analysis of the percentage of CD45RA-positive (X-axis) and/or CD45RO-positive (Y-axis) cells (n=5). **b-g**, Representative histograms and statistical analysis of CD69 (**b**), CD62 (**c**), CD107 (**d**), HLA-DR (**e**), cleaved caspase-3 (**f**) and viability (Annexin V-negative population) (**g**). (**b-e**, n=5; **f**, n=1; **g**, n=3). **h**, Western blotting analysis of 40ug protein extracts from 5 different time points in the cells at the end of immune response probed for Noxa and cleaved Caspase-3. β-Actin was used as a loading control

memory phenotype around d14 after stimulation. Thus, the data support our model (Fig 1.5) which predicts a decrease in Noxa expression at the end of the CTL phase, post-apoptosis, and total absence of the Noxa

protein in memory cells (Fig.2.4 h).

Re-stimulation of human $CD8^+$ memory T cells results in rapid and significant re-induction of the Noxa protein

Having established a timeline for the immune response in human $CD8^+$ T cells in vitro and demonstrated the emergence of a memory-like phenotype, we next tested the ability of the memory cells to respond re-stimulation as one indicator of their functional ability. The viable cell population derived from the ficoll density gradient centrifugation of d15 stimulated $CD8^+$ T cells, designated Memory unstimulated (Mem-US) cells, were compared with the pre-ficoll d15 population via flow cytometry. There were no significant differences in most activation and differentiation markers in the live, viable cells as compared to the pre-ficoll population. However, HLA-DR showed significantly higher expression level in the ficolled cells. (Fig. 2.5 a-d). To further characterize the features and responses of the memory-like human $CD8^+$ T cells in vitro, tests for stimulation and differentiation were carried out as described earlier. The recall stimulation triggered an increase in CD69 surface expression with 20 hours followed by a rapid decrease (Fig. 2.5

a). CD62L, on the other hand, showed a decreased sharply after the stimulation (Fig. 2.5 b). Appearance of CTL markers indicative of differentiation occurred around 40 hours post-stimulation (Fig. 2.5 c-d) and activation and differentiation markers decreased on d6. Surprisingly, no significant change was detected in either levels or distribution pattern of CD45RA/CD45RO following re-stimulation (Fig.2.5 e). To further characterize the human $CD8^+$ T memory cell population, we assessed the mitochondrial energy reserve of before and after re-stimulation (Fig. 2.5 f). Memory T cells have been reported to depend on OXPHOS for energy production and show a preference for fatty acid β-oxidation utilization. To meet the requirement for long-term cell survival and the ability to be swiftly activated by re-stimulation, memory T always cells exhibit augmented SRC [25, 26]. Compared with the re-stimulated human $CD8^+$ T cells, the unstimulated (Mem-US) cells maintained substantial spare respiratory capacity (SRC) in their mitochondria (Fig. 2.5 g).

Thus, the viable $CD8^+$ T cells remaining in the culture unperturbed for 15 days following co-stimulation exhibit a memory-like phenotype with respect to markers and have mitochondria with high reserve energy levels. Our model would predict rapid induction of the protein in memory cells upon re-stimulation (Fig. 1.5). The western blot (Fig. 2.5 h) shows robust and significant upregulation Noxa expression within 24 hours of re-stimulation suggesting that the cells were primed to respond rapidly to a second exposure to antigen in keeping with the memory cell phenotype.

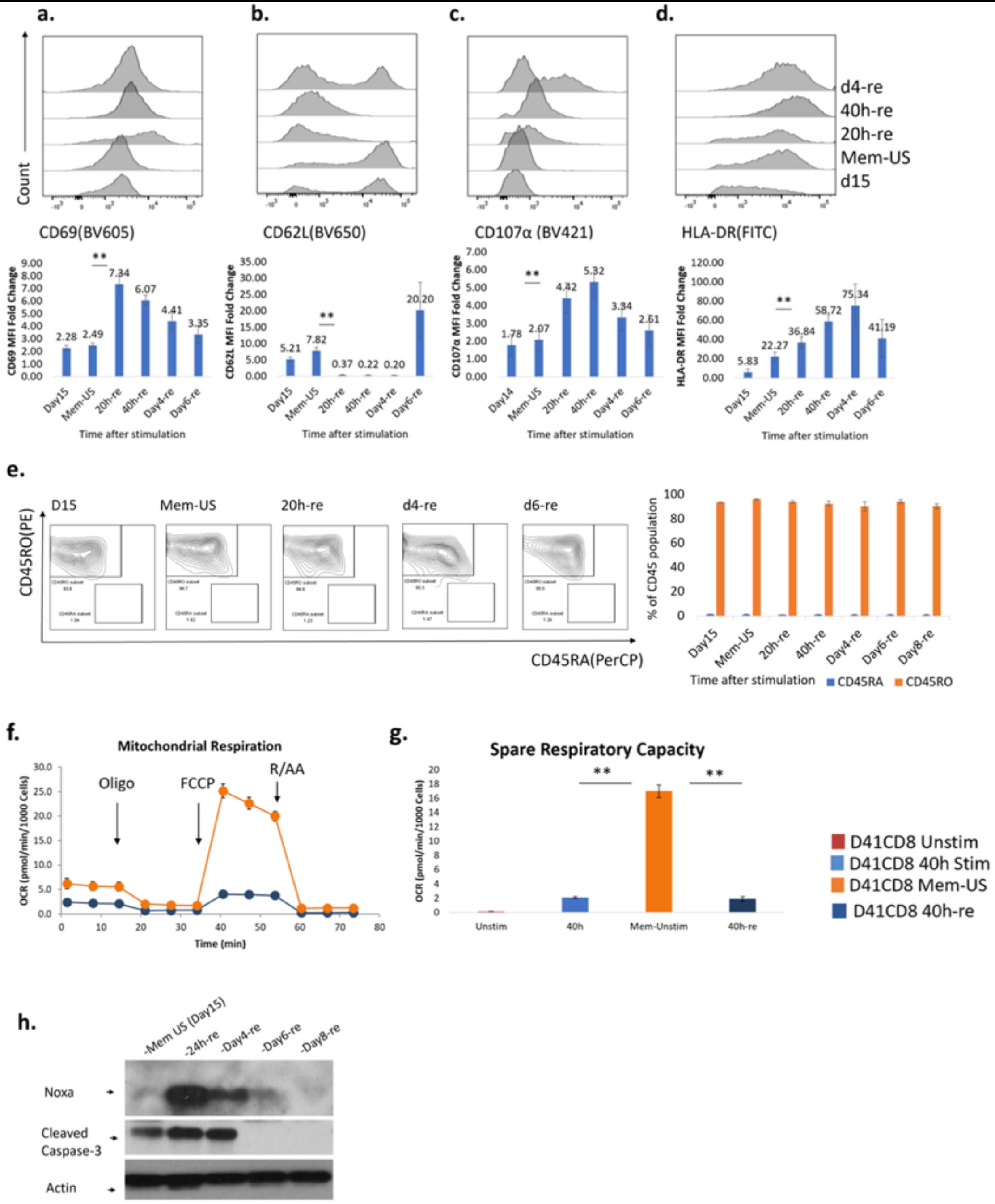

Fig 2.5| Re-stimulation of human CD8+ memory T cells rapidly induces Noxa expression. a-d, Representative histograms and statistical analysis of CD69 (**a**), CD62 (**b**), CD107 (**c**) and HLA-DR (**d**) in CD8⁺ T cells before and after re-stimulation (n=5). e, Representative contour plot and analysis of the percentage of CD45RA-positive (X-axis) and/or CD45RO-positive (Y-axis) in CD8⁺ cells before and after re-stimulation (n=5). **f,g,** Representative OCR (**f**) and spare respiratory capacity (SCR) (**g**) of human CD8⁺ T cells in a resting state, 40h after primary stimulation, unstimulated memory and memory cells 40h after recall stimulation. Oligo., oligomycin; R/AA, rotenone/antimycin. n=5 technical replicates. **h,** Western blots of protein extracts (40ug) from 5 different time points as indicated, before and after re-stimulation probed for Noxa and cleaved Caspase-3. β-Actin was used as a loading control.

Based on our observations, we divide the immune response of human CD8^{+} T cells in vitro broadly into 5 phases (Fig 2.6): Phase Ⅰ (d0), the unstimulated phase, in which cells were assumed to be naïve T cells and no Noxa was detected in the cells. Phase Ⅱ (d0-d4), the early activation of CD8^{+} T cells in which Noxa expression was induced in response to antigenic stimulation. Phase Ⅲ (d4-d10) the effector phase, in which cells differentiated into CTLs or effector-like cells and continued to express high levels of Noxa, before succumbing to apoptosis. Phase Ⅳ (d10-d14) the memory phase, in which the small percentage of remaining viable cells became quiescent memory-like T cells, losing all Noxa expression. Finally, phase Ⅴ (d14-40h-re) was the re-stimulation of the memory T cells, where the activation and induction of Noxa expression was more rapid and robust than the primary stimulation.

ATAC-seq testing in human CD8^{+} T cells immune response

Preliminary studies with CD3^{+} human T cells had determined that Noxa protein was transcriptionally induced upon co-stimulation. Our model in Figure 1.5 predicts that high Noxa protein expression is associated with antigenically stimulated, actively proliferating cells, that Noxa is required for apoptosis at the end of the immune response and that naïve and memory T cells downregulate or lack Noxa protein expression, in keeping with Noxa's role in proliferative metabolism. Results described in this section largely support the model (see western blot in Fig. 2.6). Thus, Noxa would be predicted to be tightly regulated at the gene level during a typical immune response. To determine whether chromatin accessibility in the genome region surrounding *PMAIP* (human *Noxa*) gene[4] and promoter changes through the duration of the immune response, we subjected genomic DNA from 5 different time points (see Table 2.1) to ATAC-seq [27, 28] surmising that stimulation and re-stimulation would detect open chromatin while the *PMAIP* promoter would be inaccessible in unstimulated primary and memory CD8^{+}T cells (Fig 2.7). High quality 15 dual-indexed ATAC-Seq libraries were created based on the transposed DNA and run by NovaSeq. The accessible genes were identified by peak caller. Several specific marker gene peaks, including those from CD69 and GZMB (granzyme B), were not detected in unstimulated cells but showed up in early activated CD8^{+} T cells, serving as positive controls for activation and CTL differentiation. Gene peaks for PMAIP increased in number after TCR stimulation and then decreased to the lowest level in Mem-US, increasing again following the recall stimulation. All detected PMAIP gene peaks shared an Ensembl ID confirming they were read from the same gene. However, two kinds of peaks, PMAIP1 Peak1 and Peak2, were identified based on the gene length and transcript IDs (Table 2.3 a.). PMAIP Peak1 was detected in all samples all the time and the number of identified PMAIP peak1 was stable at different time points. The number and frequency of PMAIP Peak2 corresponded with Noxa protein expression in the cells, increasing after

TCR stimulation/re-stimulation and not detected in the Mem-US (Table 2.3 b.).

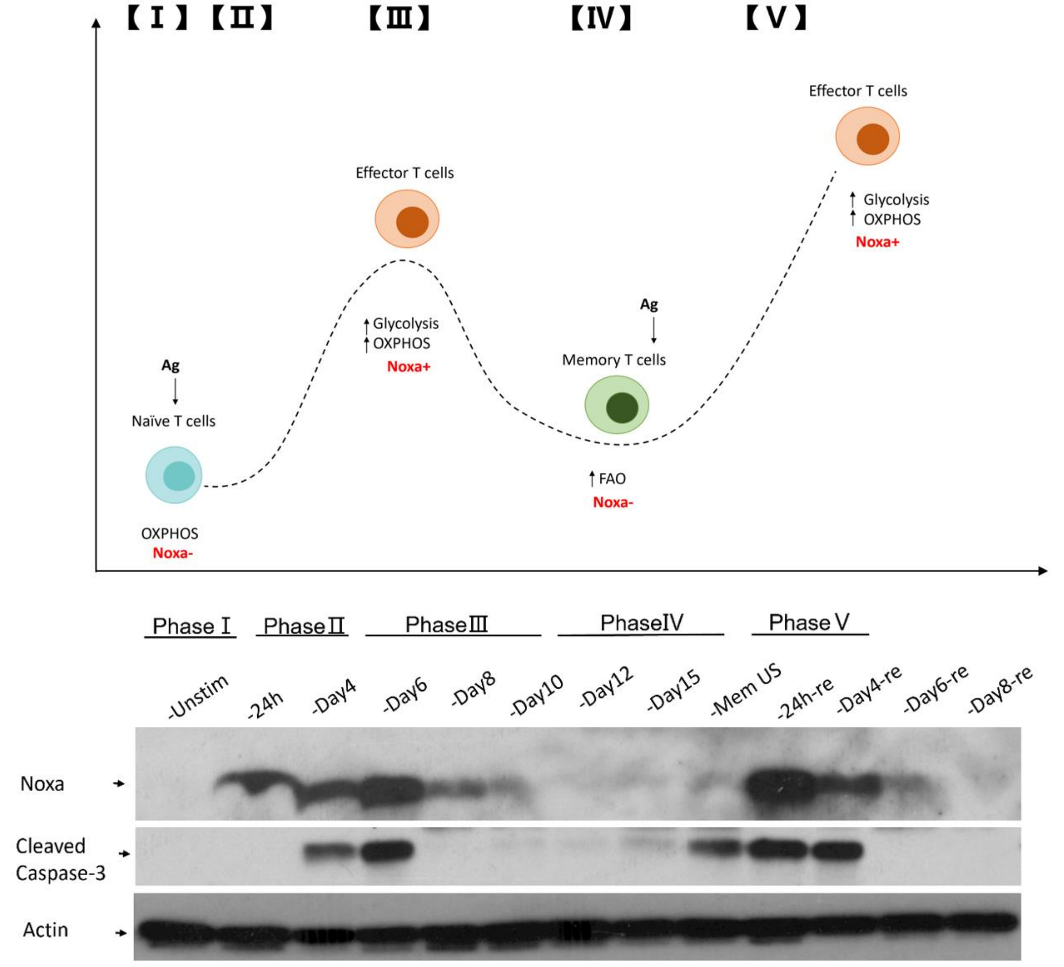

Fig 2.6| Five discernible phases in the in vitro human CD8+ T cell immune response (top) with corresponding Noxa expression (bottom).

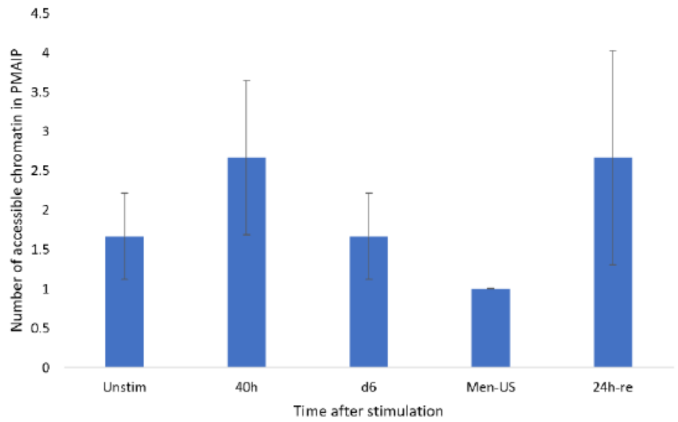

Fig 2.7| The number of accessible PMAIP gene at different time points. DNA from 3 donors were tested at the same 5 time points after antigenic stimulation. Represetative data of the accessible PMAIP gene at different time points. n=3, Error bars indicate the mean±s.e.m.

a.

Peak	ENSEMBL	SYMBOL	Gene Length	transcript-ID
Peak1	ENSG00000141682	PMAIP1	4359	ENST00000316660.6
Peak2	ENSG00000141682	PMAIP1	2928	ENST00000590596.1

b.

	D17		D25		D36	
	Peak1	Peak2	Peak1	Peak2	Peak1	Peak2
Unstim	1	0	1	0	2	1
40h	1	1	1	0	2	3
d6	1	0	1	1	1	0
Mem-US	1	0	1	0	1	0
24h-re	1	0	1	0	3	3

Table 2.3| The ATAC-seq annotation of *PMAIP*. a,Two different peaks of *PMAIP* and corresponding gene length and transcript IDs (ENST: beginning code with human transcripts). **b,** the number of identified peak tested in the *PMAIP* gene in 3 donors during the immune response at specific time points.

Generation of *Noxa* knockout (KO) CD8$^+$T cells to investigate the role of Noxa in the immune response

To validate results from our studies described earlier in this chapter and to further investigate the contribution of Noxa to the CD8$^+$ T cell immune response in the proliferation, differentiation and apoptotic phases, we generated *Noxa* KO human CD8$^+$ T cells via CRISPR/Cas9 sgRNA editing in vitro. Knockout was confirmed in western blots of early as well as late passage transfectants prior to characterization (Fig.2.8 a). The response of *Noxa* KO or Cas9-control human CD8$^+$ T cells co-stimulated in vitro was analyzed by flow cytometry. A striking difference that emerged from our preliminary studies was that a higher percentage of live cells remained at the end of immune response in the KO population (Fig.2.8 b), suggesting that knockout of Noxa reduced apoptosis of activated CD8$^+$ T cells. Two markers of activation, CD69 and CD25, were detected at significantly higher intensity on NKO cells on d4 after stimulation compared with the control group (Fig.2.8 c and d), although both these differences were not retained at later time points after stimulation. Additionally, Noxa KO cell mitochondria displayed lower SRC that control cells before stimulation, although both OCR and SRC increased significantly compared to Cas9 controls in 24h stimulated Noxa KO cells (Fig.2.8 j-k). These results suggest that Noxa could modulate early activation in human CD8$^+$ T cells but will need to be further investigated. The expression pattern of CD127/KLRG1 used for evaluation possible differences in short-lived effector cell (SLECs) and memory precursor cell differentiation (MPECs) between the Noxa KO and Cas9 cells failed to reveal any differences (Fig.2.8 e-f). Neither did we identify significant differences in proliferation rates between Noxa KO cells and Cas9 controls shortly after stimulation (Fig.2.8 g). Preliminary conclusions are (a) that Noxa may modulate or temper the activation response in human $CD8^+$ T cells and (b) that Noxa may be required for apoptosis at the end of the immune response.

Noxa has been reported to play a critical role in regulating glutamine utilization for the mitochondrial TCA cycle [6, 8]. Preliminary studies have also suggested that Noxa is required for the metabolic switch to glutaminolysis in activated primary T cells (Benson and Kelekar, unpublished). Although no significant differences were detected between Noxa KO and Cas9-control cells cultured and activated in normal glutamine-rich medium, Noxa-deficient mitochondria showed higher TMRE (tetramethylrhodamine ethyl ester) labeling compared to the Cas9-controls after 24h stimulation in the absence of glutamine, suggesting greater mitochondrial fitness and lower dependence on glutamine for respiration (Fig.2.8 h-i).

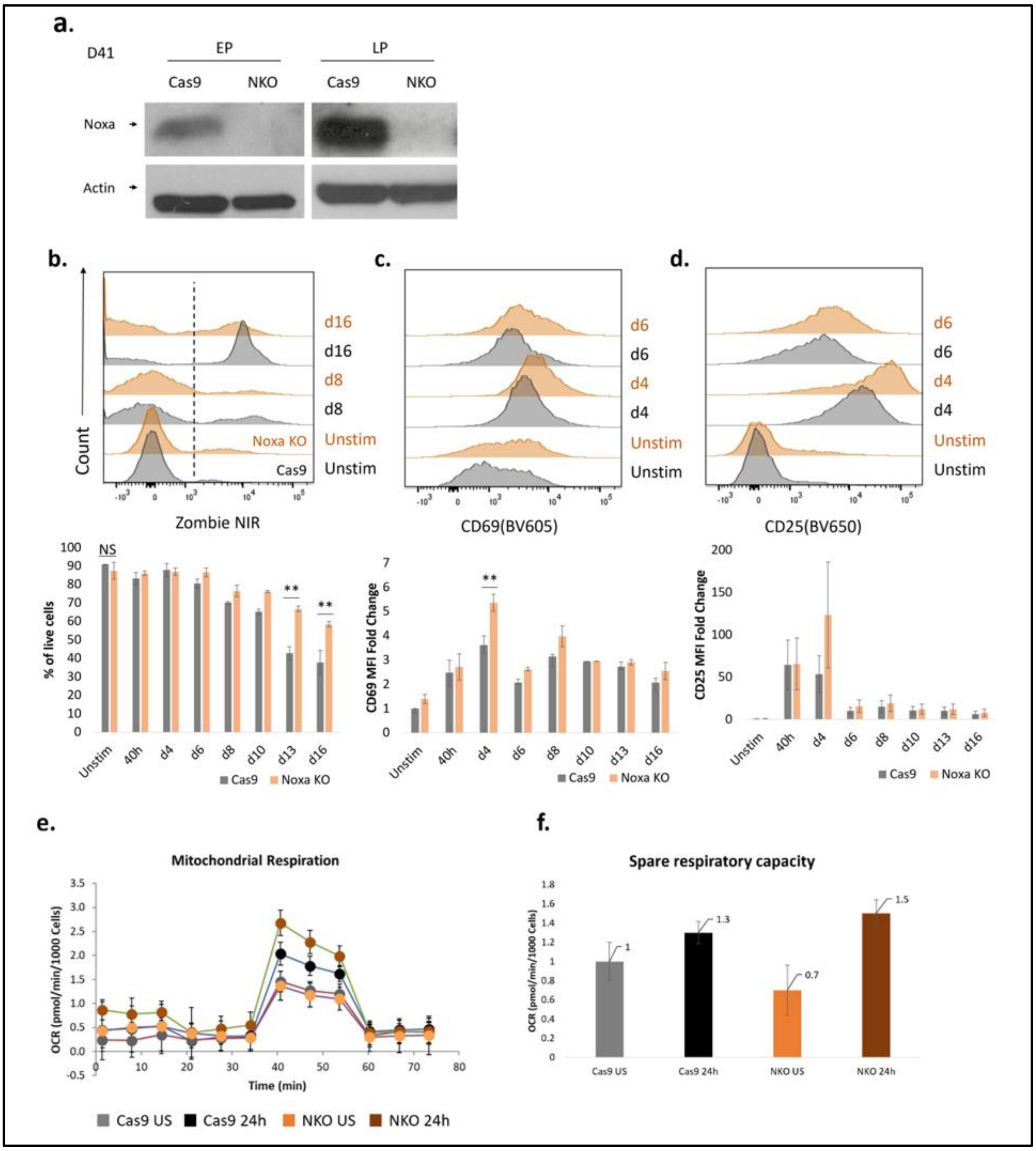

a.
D41
EP
LP
Cas9
NKO
Cas9
NKO
Noxa
Actin
b.
d16
d16
d8
d8
Noxa KO
Unstim
Cas9
Unstim
Count
Zombie NIR
c.
d6
d6
d4
d4
Unstim
Unstim
CD69(BV605)
d.
d6
d6
d4
d4
Unstim
Unstim
CD25(BV650)
% of live cells
NS
**
**
Unstim
40h
d4
d6
d8
d10
d13
d16
Cas9
Noxa KO
CD69 MFI Fold Change
**
CD25 MFI Fold Change
e.
Mitochondrial Respiration
OCR (pmol/min/1000 Cells)
Time (min)
Cas9 US
Cas9 24h
NKO US
NKO 24h
f.
Spare respiratory capacity
OCR (pmol/min/1000 Cells)
1
1.3
0.7
1.5
Cas9 US
Cas9 24h
NKO US
NKO 24h

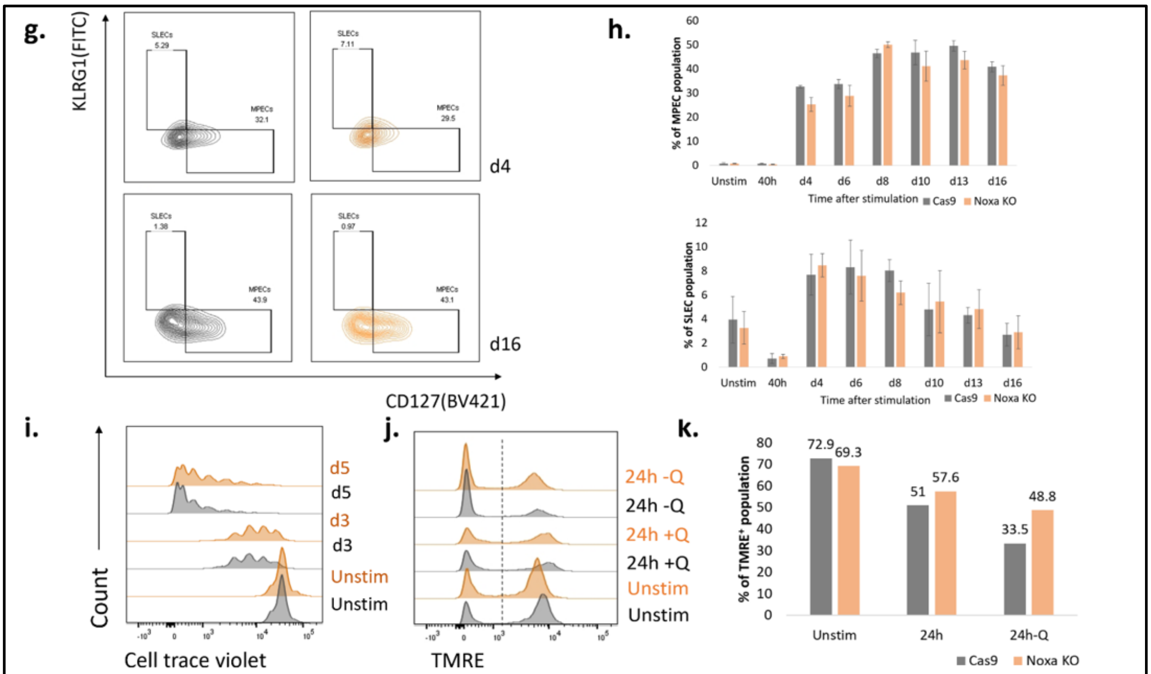

Fig.2.8| Human Noxa may modulate early activation and mitochondrial fitness of stimulated CD8+T cells and be required for apoptosis at the end of the immune response in vitro. Noxa knockout (KO) CD8$^+$ cells were generated via CRISPR/Cas9 sgRNA editing. **a,** Western blotting of Noxa KO and Cas9-control cells 48h after stimulation early and late passage transfectants (EP: early passage, LP: late passage)**. b-d**, Representative histograms, percentage of cell population and MFI fold change of live cells (**c**) (left part of the gate), CD69 (**c**) and CD25(**d**) in Cas9 control cells(grey) and Noxa KO cells (orange). Error bars indicate the mean±s.e.m. n=2. **e,f,** OCR (**e**) and spare respiratory capcity (SCR) (**f**) of transfected human CD8+ T cells in resting and 40h after anti-CD3/CD28 stimulation. Oligo., oligomycin; R/AA, rotenone/antimycin. Metabolic data were from 5 technical replicates from a single donor. **g, h,** Representative contour plot (**g**) and percentage of cells population (**h**) for SLECs and MPECs based on KLRG1/CD127 expression pattern at different time points after stimulation in Cas9 control cells(grey) and Noxa KO cells (orange). (SLECs: KLRG1$^+$/CD127$^-$, MPECs: KLRG1$^-$/CD127$^+$) **i.** the histogram of CTV compared in Cas9 control and Noxa KO cells after stimulation. **j,k**, Cas9 and Noxa KO cells were activated in normal glutamine-rich medium (2mM) (+Q) or in the absence of glutamine (-Q) for 24h. Representative TMRE (tetramethyl rhodamine, ethyl ester) histograms(**j**) and percentage of TMRE$^+$ cells in the population (right part of the gate)(**k**) in the cells. n=2, error bars indicate the mean±s.e.m. **p≤0.01.

Chapter 3: Discussion

In this dissertation we have developed an in vitro activation model using primary human CD8$^+$ T cells to investigate the contribution of human Bcl-2 protein Noxa to the immune response. The metabolism of activated T cells is reprogrammed to support the rapid proliferative burst that precedes their differentiation into effector and memory T cells[22, 23, 29]. The increased glucose uptake serves to provide glucose carbons for producing building blocks for biomass and activated T cells switch to glutamine as the primary carbon source for OXPHOS and energy generation. Human Noxa, a BH3-only protein, was previously shown to have pro-apoptotic as well as pro-growth functions and to promote both aerobic glycolysis and glutaminolysis in transformed and normal T cells [3, 6, 8]. The goal of my thesis research was to test the hypothesis that Noxa was required not only for the metabolic reprogramming in activated human T cells but also for the expansion and the apoptotic phases of an immune response.

These studies show, for the first time, that Noxa was rapidly induced in CD8$^+$T cells upon TCR stimulation and remained highly expressed in proliferating effector cells (CTLs) through apoptosis. Cells remaining at the end of the effector phase displayed distinct memory phenotypes and lacked Noxa protein expression but could be induced to rapidly upregulate Noxa upon re-stimulation (Fig 2.6). Although more experiments needed to be done for validation, our work clearly suggests that Noxa plays an important role in glutamine utilization for energy production and regulating progress of CD8$^+$ T cells through apoptosis and is either not required or inhibitory for memory cell generation.

While our studies confirm Noxa's role in proliferative metabolism previously identified in leukemia cells, they also offer novel insights into the protein's contribution to several phases of a normal immune response of a T cell. For instance, just as the pro-survival phosphorylated form of Noxa in Jurkat T cells was shown to be localized within a multiprotein complex and inaccessible to immunoprecipitating antibodies[6], Noxa induced after antigenic stimulation of $CD8^+$T cells could be detected in a western blot but not in an IP/Western. However, again, as in the T leukemia study, Noxa could be immunoprecipitated from apoptotic cells (Fig 2.3.i)[6], These results support a pro-growth function for induced Noxa in proliferating T cells and suggest that it is sequestered in a protein complex.

Novel insights into the memory phenotype have emerged from our studies. Despite its limitations, the in vitro immune response assay not only allowed us to follow $CD8^+$T cell activation and differentiation through to apoptosis but also enabled isolation and characterization of memory-like cells that responded robustly to re-stimulation. The persistence of CD45RO positivity, a distinguishing feature of memory T cells, after d4 and the absence of CD45RA expression in re-activated cells, was unexpected and suggests that CD45RO may work as a marker of cells that have encountered antigens. The robust re-stimulation of memory like $CD8^+$ T cells supported the ability of these cells to provide rapid protection and require a lower threshold for enhanced function.

While no significant differences were detected in KLRG1/CD127 pattern in differentiating Noxa KO CD8$^+$T cells compared to controls, the higher viability of Noxa knockout cells at the end of the activation assay strongly support a role for Noxa during the apoptotic phase. It has been well documented that the CD8$^+$ T cell differentiation is highly dependent on the cytokine IL-2. The IL-2 receptor, CD25, is a marker for early activation in T cells. Additionally, cells with low CD25 expression showed reduced sensitivity to IL-2 and become memory T cells. Overall, we did not observe significant differences in CD25 expression in the late activation phase with the deletion of Noxa. Thus, Noxa enhanced cell viability without affecting T cell differentiation characteristics, which makes the protein an attractive target for an immunotherapeutic approach aimed at rescuing T cells with a more pronounced response to activating antigens.

Although much remains to be investigated regarding the role of Noxa in T cell development, the results obtained from our in vitro model of the human CD8$^+$ T cell immune response allow us to conclude the following: Noxa makes important contributions not only to the metabolic reprogramming and proliferation that occurs early in antigenically stimulated human CD8$^+$ T cells, but also to their functional differentiation to effector cells and to the apoptosis that occurs at the culmination of the immune response.

Chapter 4: Materials and Methods

Primary T-cell cultures.

Human peripheral blood mononuclear cells (PBMCs) were obtained from Memorial Blood Center, St. Paul, MN, USA and isolated from whole blood (10 min, 25°C, 900 g without break) over Histopaque®-1077 (density 1.077 g/mL, Sigma Alrich) . After 18 hours resting in ImmunoCult™-XF T Cell Expansion Medium (STEMCELL Technologies, no. 10981), live PBMCs were purified bydensity gradient centrifugation (25 min, 25°C, 1000 g without break) over Ficoll - Paque™ PLUS (density 1.077 g/mL, Cytiva) and allowed to rest for 2 hours in ImmunoCult™-XF T Cell Expansion Medium. Human $CD8^+$ T cells were isolated via using the EasySepTM human $CD8^+$ T-cell isolation kit (STEMCELL Technologies, no.17953) according to the manufacture's protocol. human $CD8^+$ T cells were activated in media at a density of 1x106 cells /ml by adding ImmunoCult Human CD3/CD28 T Cell Activator (STEMCELL Technologies, no.10791) (25ul/ml) and IL-2 (Peprotech) at a final concentration of 4 ng/mL (66 IU/ng). .

Generation of human $CD8^+$ memory T cells and re-stimulation.

One group human $CD8^+$ T cells were set aside for memory cells formation. Human $CD8^+$ T cells were activated as described above and cultured without disturbance. Media was added when necessary. 14 days after stimulation, human $CD8^+$ memory T cells were purified by density gradient centrifugation with Ficoll - Paque™ PLUS as previously described and allowed to rest for 2 hours in ImmunoCult™-XF T Cell

Expansion Medium. The remaining human $CD8^+$ T cells were used as memory like T cells and were activated again as described above for further testiing.

Western blotting

Cells were washed with cold PBS once and lysed in RIPA buffer (50mM Tris-HCl [pH7.5]), 150mM NaCl, 0.5% v/v sodium deoxycholate, 1% v/v Nonidet P-40, 0.1% SDS) supplemented with protease (Inhibitor Cocktail III, Calbiochem) and phosphatase (inhibitor cocktail III, Millipore) inhibitor cocktails, followed by centrifugation at 10,000rpm for 10 min at 4 °C. 40ug protein lysate was denatured with 2x Laemmli buffer (Biorad, no. 1610737) for 3 min at 85°C. Protein lysates were resolved by SDS-PAGE, transferred to nitrocellulose membrane. Membranes were blocked with TBS-TM (20 mM Tris-HCl pH 7.6, 37 mM NaCl, 0.1% Tween 20®, 5% skim milk) and incubated with the appropriate antibodies in TBS-Tat 4°C overnight. Primary antibodies were used at the following dilutions: β-Actin (1:7000) (Santa Cruz Biotechnology, no. sc-69879), Mcl-1(1:1000) (Cell Signaling Technologies, no. 94296S), Cleaved Caspase-3 (1:1000) (Cell Signaling Technologies, no. 9664S)and Noxa (1:500 – 1:1000) (Cell Signaling Technologies, no. 14766S). After 1h incubation with secondary HRP-conjugated antibody (Invitrogen) in TBS-TM, chemiluminescence reactions carried out using the Pierce ECL Western Blotting Substrate (Thermo Scientific), ProSignal Pico or Femto ECL Reagent Kits (Prometheus). Blots were stripped for reuse by washing for 5 minutes in TBS-T buffer (pH 2.5-3.0) before re-blocking with TBS-TM

Immunoprecipitation

Cells were washed with cold PBS once and lysed in Dignam Buffer A (10mM HEPES, 0.015mM MgCl2, 10mM KCl, 0.05% IGEPAL) supplemented with protease and phosphatase inhibitor cocktails. 200-300ug protein lysate was incubated with 2-3ug anti-Noxa antibody (Cell Signaling Technology, no. 14766) at 4°C overnight. The antibody-protein complex was captured on ProteinG-Agarose beads (Invitrogen). Immunoprecipitates were resolved by SDS-PAGE and detected by western blotting as described earlier

CRISPR/Cas9 Genomic Editing

$2x10^6$ human $CD8^+$T cells were activated and cultured in ImmunoCult™-XF T Cell Expansion Medium (STEMCELL Technologies, no. 10981) for 48 h prior transfection with sgRNAs.) sgRNAs targeting PMAIP1 (Noxa) sequence: CACCGGCGGAGAUGCCU – Modified were obtained from Synthego (catalog: $PMAIP1^+59900181$) and Clean Cap 3XNLS Cas9 mRNAs were obtained from TriLink (no. L-606-100). Briefly, 100pmol sgRNAs were incubated with 1ug of Cas9 Nuclease for 10-15 min at room temperature. Preactivated CD8⁺ T cells were washed once in cold PBS and resuspended in 19.5 ul T buffer (Invitrogen). Neon Transfection System (Invitrogen) was used for the transfection experiments and each set of experiments was conducted via the 10ul tips (Invitrogen). 1400 Volts, 10 pulse widths, 3 pulses were the setting for the parameters. After transfection, the cells were transferred to 1ml T cell expansion basal medium (TCEM), with Optimizer CTS (Gibco), CTS Immune Cell SR (Gibco), 2mM L-Glutamine (VWR Life Science). 100U/ml penicillin, 100μg/ml streptomycin (Gibco) were added 48h after transfection.

Flow cytometry (surface and intracellular staining)

500,000 human $CD8^+$ T cells single-cell suspensions were obtained at different time points after stimulation and analyzed by flow cytometry. Cells were surface stained with anti-CD8α (BioLegend, Brilliant Violet 785™, RPA-T8, no. 301046), anti-CD69 (BioLegend, Brilliant Violet 605™, FN50, no. 310938), anti-CD25 (BioLegend, Brilliant Violet 650™, BC96, no. 302634), anti-CD62L (BioLegend, Brilliant Violet 650™, DREG-56, no. 304832), anti-CD107α (BioLegend, Brilliant Violet 421™, H4A3, no. 328626), anti-HLA-DR (BioLegend, FITC, LN3, no. 327006), anti-CD45RA (BioLegend, PerCP, HI100, no. 304155), anti-CD45RO (BioLegend, PE, UCHL1, no. 304206), anti-CD127 (BioLegend, Brilliant Violet 605™, A019D5, no. 351334), anti-KLRG1 (BioLegend, FITC, 2F1/KLRG1, no.138410) and Zombie NIR™ (BioLegend, no.

423106). CellTrace™ Violet Cell Proliferation Kit (Thermo Scientific, no. C34571) was used for proliferation staining following the manufacture's protocol.

For intracellular staining, cells were first fixed with 1X FoxP3/Transcription Factor Fixation/Permeabilization Buffer (Cell Signaling Technology, no. 43481) for 1 hour at RT in the dark. Antibodies were diluted in 1X FoxP3/Transcription Factor Permeabilization Buffer (Cell Signaling Technology, no. 43481) and incubated for 1 hour at RT protected from light. Cells were washed twice with 1X FoxP3/Transcription Factor Permeabilization Buffer. Supernatant was discarded before cells were resuspended in 200-500 µl 1X FoxP3/Transcription Factor Permeabilization Buffer and taken to flow for analysis.

Flow cytometry was performed on a BD LSR II flow cytometer and the data were analyzed using Flowjo version 10.7.1.

Mito stress test (Seahorse assays).

Real-time oxygen consumption rate (OCR) and extracellular acidification rate (ECAR) were measured using a Seahorse XFe96 Extracellular Flux Analyzer (Agilent). The day before the experiment, 200ul of water (HyClone) was added per well to hydrate the Seahorse cartridge and the cartridge was stored in a 37°C CO_2-free incubator overnight. On the experiment day, water in the plate was replaced with XF calibrant (pH=7.4, Agilent). Cells were washed once in PBS and resuspended with Seahorse

Medium pH 7.4 (Agilent), supplemented with 10mM Glucose (Agilent), 2mM Sodium Pyruvate (Agilent), and 2mM Glutamine (Agilent). Around 2 × 105 $CD8^+$ T cells per well were seeded Cell-Tak (Corning) coated 96 well plate (Agilent) in Seahorse medium. The cells were spun down to the bottom and incubated at 37 °C for a minimum of 45 min in a CO2-free incubator before starting the experiment. Mito stress test Drugs were prepared in Seahorse media accordingly: Oligomycin (ATP synthase inhibitor) 1.5μM, FCCP (Carbonyl cyanide-4 (trifluoromethoxy) phenylhydrazone) 2.0μM, collapsing the proton gradient, Rotenone/ Antimycin A 0.5μM, inhibiting mitochondria complex I/III. 1:500 Hoescht 33342 (AnaSpec.) was added to seahorse media after finishing the measurement for all treatments. Each treatment was measured 3 times after the injection of drugs. Basal OCR was calculated via the tested OCR before any treatment reducing the OCR after Rotenone/ Antimycin A treatment. The maximum OCR was obtained by subtracting the OCR after Rotenone/ Antimycin A treatment from the OCR measured in the FCCP treatment. The spare respiratory capacity was calculated via subtracting the basal OCR from the maximum OCR. Cell normalization was calculated by the cell count detected via the brightfield scan before the experiment and the fluorescent scan after the completion of the experiment by Cyation 1 platereader (Biotek).

ATAC-seq

2×10^5 $CD8^+$ T cells were harvested and washed once with cold PBS. Cell pellet was gently resuspended in 200µl of cold lysis buffer (10 mM Tris-HCl, pH 7.4, 10 mM NaCl, 3 mM MgCl2 and 0.1% IGEPAL CA-630). Took 50ul of cell suspension, spun down immediately at 500 ×g for 10 min, 4°C and discard the supernatant. The cell pellet was set on ice and resuspended with transposition reaction mix including: 25 µl TD (2x reaction buffer), 2.5 µl TDE1 (Nextera Tn5 Transposase) and 22.5 µl Nuclease Free H2O. The transposition reaction was incubated at 37°C for 30 min with gentle mixing. The DNA was purified via Qiagen MinElute PCR Purification Kit and stored at −20°C before sequencing -

References:

1. Hijikata, M., et al., *Molecular cloning and characterization of a cDNA for a novel phorbol-12-myristate-13-acetate-responsive gene that is highly expressed in an adult T-cell leukemia cell line.* J Virol, 1990. **64**(10): p. 4632-9.
2. Giam, M., D.C. Huang, and P. Bouillet, *BH3-only proteins and their roles in programmed cell death.* Oncogene, 2008. **27 Suppl 1**: p. S128-36.
3. Hershko, T. and D. Ginsberg, *Up-regulation of Bcl-2 homology 3 (BH3)-only proteins by E2F1 mediates apoptosis.* J Biol Chem, 2004. **279**(10): p. 8627-34.
4. Ploner, C., R. Kofler, and A. Villunger, *Noxa: at the tip of the balance between life and death.* Oncogene, 2008. **27 Suppl 1**: p. S84-92.
5. Warr, M.R. and G.C. Shore, *Unique biology of Mcl-1: therapeutic opportunities in cancer.* Curr Mol Med, 2008. **8**(2): p. 138-47.
6. Lowman, X.H., et al., *The proapoptotic function of Noxa in human leukemia cells is regulated by the kinase Cdk5 and by glucose.* Mol Cell, 2010. **40**(5): p. 823-33.
7. Karim, C.B., et al., *Structural Mechanism for Regulation of Bcl-2 protein Noxa by phosphorylation.* Sci Rep, 2015. **5**: p. 14557.
8. Hanse, E.A., et al., *Cytosolic malate dehydrogenase activity helps support glycolysis in actively proliferating cells and cancer.* Oncogene, 2017. **36**(27): p. 3915-3924.
9. Wensveen, F.M., et al., *Apoptosis threshold set by Noxa and Mcl-1 after T cell activation regulates competitive selection of high-affinity clones.* Immunity, 2010. **32**(6): p. 754-65.
10. Raff, M.C., *T and B lymphocytes and immune responses.* Nature, 1973. **242**(5392): p. 19-23.
11. Whitacre, J.M., J. Lin, and A. Harding, *T Cell Adaptive Immunity Proceeds through Environment-Induced Adaptation from the Exposure of Cryptic Genetic Variation.* Front Genet, 2012. **3**: p. 5.
12. Williams, M.A. and M.J. Bevan, *Effector and memory CTL differentiation.* Annu Rev Immunol, 2007. **25**: p. 171-92.
13. Hassin, D., et al., *Cytotoxic T lymphocyte perforin and Fas ligand working in concert even when Fas ligand lytic action is still not detectable.* Immunology, 2011. **133**(2): p. 190-6.

14. Mosmann, T.R., et al., *Two types of murine helper T cell clone. I. Definition according to profiles of lymphokine activities and secreted proteins.* J Immunol, 1986. **136**(7): p. 2348-57.

15. Swain, S.L., K.K. McKinstry, and T.M. Strutt, *Expanding roles for CD4(+) T cells in immunity to viruses.* Nat Rev Immunol, 2012. **12**(2): p. 136-48.

16. Piccirillo, C.A., *Regulatory T cells in health and disease.* Cytokine, 2008. **43**(3): p. 395-401.

17. Cluxton, D., et al., *Differential Regulation of Human Treg and Th17 Cells by Fatty Acid Synthesis and Glycolysis.* Front Immunol, 2019. **10**: p. 115.

18. Zhang, N., et al., *The role of apoptosis in the development and function of T lymphocytes.* Cell Res, 2005. **15**(10): p. 749-69.

19. Marsden, V.S. and A. Strasser, *Control of apoptosis in the immune system: Bcl-2, BH3-only proteins and more.* Annu Rev Immunol, 2003. **21**: p. 71-105.

20. Fischer, S.F., G.T. Belz, and A. Strasser, *BH3-only protein Puma contributes to death of antigen-specific T cells during shutdown of an immune response to acute viral infection.* Proc Natl Acad Sci U S A, 2008. **105**(8): p. 3035-40.

21. Pellegrini, M., et al., *Shutdown of an acute T cell immune response to viral infection is mediated by the proapoptotic Bcl-2 homology 3-only protein Bim.* Proc Natl Acad Sci U S A, 2003. **100**(24): p. 14175-80.

22. Wang, R. and D.R. Green, *Metabolic checkpoints in activated T cells.* Nat Immunol, 2012. **13**(10): p. 907-15.

23. MacIver, N.J., R.D. Michalek, and J.C. Rathmell, *Metabolic regulation of T lymphocytes.* Annu Rev Immunol, 2013. **31**: p. 259-83.

24. Alves, N.L., et al., *The Noxa/Mcl-1 axis regulates susceptibility to apoptosis under glucose limitation in dividing T cells.* Immunity, 2006. **24**(6): p. 703-716.

25. Li, W. and L. Zhang, *Rewiring Mitochondrial Metabolism for CD8(+) T Cell Memory Formation and Effective Cancer Immunotherapy.* Front Immunol, 2020. **11**: p. 1834.

26. van der Windt, G.J., et al., *Mitochondrial respiratory capacity is a critical regulator of $CD8^+$ T cell memory development.* Immunity, 2012. **36**(1): p. 68-78.

27. Buenrostro, J.D., et al., *ATAC-seq: A Method for Assaying Chromatin Accessibility Genome-Wide.*

Curr Protoc Mol Biol, 2015. **109**: p. 21 29 1-21 29 9.

28. Sun, Y., N. Miao, and T. Sun, *Detect accessible chromatin using ATAC-sequencing, from principle to applications.* Hereditas, 2019. **156**: p. 29.

29. van der Windt, G.J. and E.L. Pearce, *Metabolic switching and fuel choice during T-cell differentiation and memory development.* Immunol Rev, 2012. **249**(1): p. 27-42.